

ES2C5 2nd-Year Laboratory

Wind Tunnel Lab Report

Student ID: 1922672

1. Abstract

We analysis the drag forces acting on the curvature section of a cylinder in the flow by doing laboratory experiments and numerical simulations. There are sections A and B, which are different in methods with different quantities measured, but aiming at the same goal. Wind tunnel is used in both section to imitate the relative velocity between fluid and sample.

Section A was carried out in a low-speed wind tunnel with cross sectional area 1.425 square meter of the working section, with a circular cylinder of diameter 113 mm mounted horizontally in it. Section B was carried out in a wind tunnel with a cross sectional area approximately 0.0169 square meter. A circular cylinder of diameter 12 mm is mounted horizontally in it at a height of 60mm above floor.

Since different methods were used, there would be noticeable differences in the results. Two Matlab codes were used comprehensively for data analysis of section A and B. It is concluded that the wake behind the testing model has significant impact on drags. Drag is also positively related to the flow speed and negatively related to the Reynolds number.

2. Introduction

It would be useful in engineering application if we could find the relationship of the drag force of an object in a liquid and other factors. The aim of this Wind Tunnel experiment is to analysis how the drag forces behaves that act on bodies in any fluid. Forces would depend on the flow speed, the body shape and consequently the flow pattern surrounding the body. It is evident form the experiment that it is the flow structure in the wake behind the testing model that has significant impact in determining the drag forces that resists the motion of the object. To simplify the flowing problem, uniformed cylinder was used as tested sample, thus the simulation and calculation were feasible to be done.

To gain a further knowledge of how the theories and backgrounds of boundary layer conditions and flow mechanisms, Chapter Six and Eight from D.J. Tritton's book, *Physical Fluid Dynamics 2nd edition* (1988), would be recommended to read.

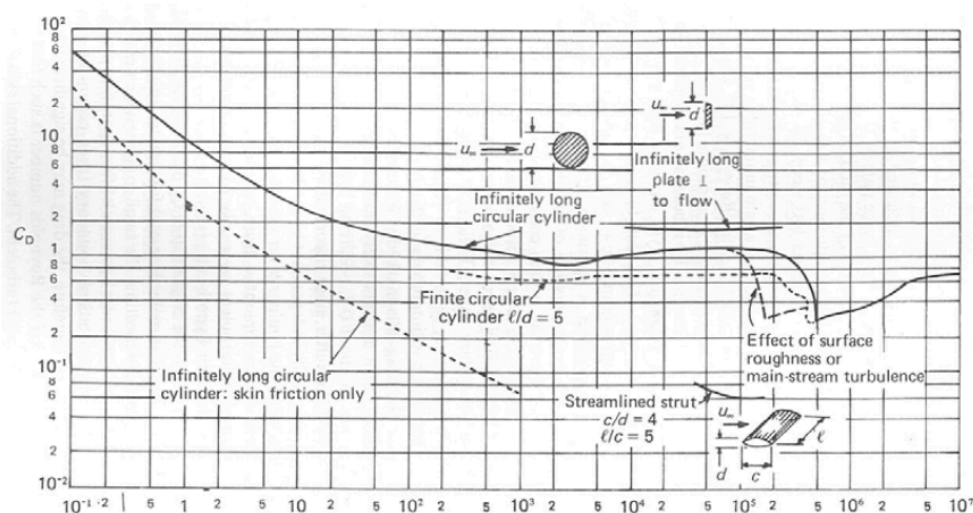


Figure 2.1: Drag coefficient for two-dimensional bodies.

2.1.General Introduction of Section A

In section A, the pressure distribution around a circular cylinder exposed to a uniform air flow was investigated. The experiment was carried out in a large low-speed wind tunnel. Some pressure measurements were taken by a multi-tube water manometer, which was connected to pressure tapings on the surface of the cylinder. Mean values were taken to make sure each measurement was accurate. Static pressure in the free upstream of the cylinder was also measured by a Pitot probe connected to the manometer. For each flow conditions with different flow rate, three measurements were taken correspondingly, which each time has resulted in either laminar or turbulent boundary layer conditions. Using computer program, the collected pressure readings were analyzed. Pressure distributions around the cylinder were plotted, and drag coefficients were determined.

2.2.General Introduction of Section B

In section B, the profile of the flow rate in the wake of a circular cylinder was determined. A smaller wind tunnel was used for this section. It is evident that the cross-wake velocity profile could be used to find the drag force acting on the cylinder. Different pressures were measured from a Pitot probe that went through the wake. The Pitot probe was connected to a micro-manometer. The micro-manometer was used to convert the pressure data into corresponding velocity readings as part of the Bernoulli equation. Velocity datas were plotted and the drag force was calculated by taking average of a suitable numerical integration of the datas using an integration scheme as described.

3.Theory and Background Study

Streamline — Path of a particle in a fluid relative to a solid body past which the fluid is moving in laminar flow without turbulence.

Reynolds Number — Ratio of internal forces to viscous forces.

$$Re = \frac{\rho \cdot d \cdot V_{\infty}}{\mu} \quad (3.1)$$

Boundary Layer — Region close to wall, in a real fluid, where flow velocity gradually increases from zero at the wall to it free-stream value u ; boundary-layer thickness is usually defined as that thickness where flow velocity reaches 99 % of u .

Boundary Layer Separation — Boundary layer separation takes place whenever an abrupt change in either the magnitude or direction of the fluid velocity is too great for the fluid to keep to a solid surface.

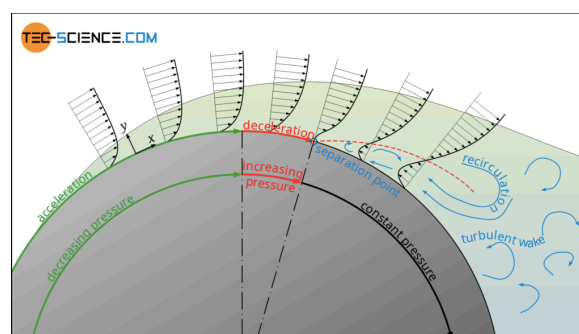


Figure3.1: Velocity distribution along a flow around a cylinder (boundary layer separation).
<https://www.tec-science.com/mechanics/gases-and-liquids/flow-separation-boundary-layer-separation/>

Skin Friction Drag — Caused by wall shear stresses that act between the fluid and the body surface due to the viscosity.

Pressure Drag — The pressure drag has its cause in the different static pressures, which act on the body due to the conservation of energy.

Drag Coefficient — The friction drag coefficient is the coefficient of the wall shear stress in relation to the flow velocity of the undisturbed external flow. This coefficient itself is dimensionless.

$$C_d = \frac{D}{\frac{1}{2} \rho \cdot v_{\infty}^2 \cdot l} \quad (3.2)$$

Pressure Coefficient — Defined as static pressure difference over dynamic pressure.

$$C_p = \frac{p - p_{\infty}}{p_d} = \frac{p - p_{\infty}}{\frac{1}{2} \rho \cdot v_{\infty}^2} \quad (3.3)$$

4. Experiment Setup

Experiments were done in wind tunnels, objected at a cylinder that cut through the wind direction. Before starting the experiments, checking and zeroing all measuring equipments would be useful. For the safety issue, it is essential to ensure all parts in the wind tunnel are fixed. The isolation window should be closed first then start the wind tunnel.

In section A, the experiment set up is provided as shown right. This is a figure taken from the wind tunnel briefing lecture's note, wt_brief_lec.pdf. The manometer used might be Longwin, LW-8007, 20-Column Liquid Manometer.

In section B, the set up is shown on the right. It is a figure for Drag of a body from wake measurement, with a Pitot-static tube.

4.1. Experiment Setup and Methodology of Part A

For part A, experiments were set up in the large low-speed wind tunnel, with cross section dimensions of 1.04m • 1.37m. There was a circular cylinder with a diameter 113mm mounted horizontally in the working section. It was assumed that end effects could be neglected, therefore the flow was basically two dimensional.

Thirteen of pressure tappings were distributed at the upper half center of the cylinder. The first tapping was accurately aligned with the free-stream direction, followings were separated evenly, and the last tapping located at the rear. Due to the flow geometrics, the pressure distribution on the lower surface was symmetrical compared to the upper. Tunnel air flow speed was measured and recorded, by a single tapping located in the free stream. Pressure was measured by them that were



Figure 4.1: Experiment set up for section A.

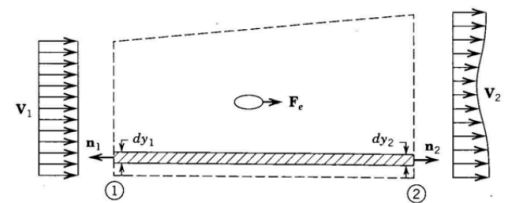


Figure 4.2: Experiment set up for section B

connected to the multi-tube water manometer. Free upstream static pressure was measured by a Pitot-static probe. The atmospheric pressure was eliminated from the data by computer program, and gauge pressure was therefore determined. Free stream dynamic pressure was the difference in reading between 0° tapping and free stream tapping.

First set of datas was collected with the wire mesh inside the tunnel and maximum wind speed, second was done with the wire removed and maximum wind speed, and third was done without the wire and half wind speed. Records of manometer tube level was taken for thirteen tappings, free stream static pressure and wind speed.

The actual reading fluctuated randomly, which could be solved by using electronic pressure sensor instead. There should be no inclination in manometer, but experiment was also applicable if the inclination remained constant through reading, as it would be cancelled out through calculation. A wire mesh was provided to disturb the flow, and simulated the effect of a higher Reynolds number by increasing the free-stream turbulence. The laminar-turbulent transition was triggered earlier as a result of this mesh.

4.2.Experiment Setup and Methodology of Part B

For section B, it was carried out in a smaller wind tunnel with a cross sectional area of approximately 130mm • 130mm. A circular cylinder with a diameter of 12mm was mounted horizontally in the center of wind tunnel. Assuming that end effects was negligible and the flow can be considered as 2-dimensional.

There was a Pitot probe moving flexible vertically only. A tapping on the wall of tunnel measured static pressure. The pressure difference between the Pitot probe and the static pressure tapping is measured from a micro-manometer, and it transferred the pressure difference directly to velocity readings, which was part of the Bernoulli equation.

Pitot probe was connected to positive pressure port, and the static pressure tapping to the negative. The instrument was set ready and zeroed, then turned on the wind tunnel. Pitot position was set at height 30mm, and wind tunnel speeds were set at 15 m/s and 10 m/s. Potentiometer was turned to right to damp the readings fluctuation for velocity. Measurement was taken between 30mm and 90mm per 2mm. The readings were random at first, but returned to relatively constant later. Errors might be conducted as the manometer's reading scale was loaded far away from the actual measured liquid height.

5.Data Analysis and Discussions

All experiment datas came from the lab datas provided. All graphs were plotted based on the datas and the same sources for drag coefficients.

5.1.Data Analysis of Part A

Wind speeds were all taken down, and Reynolds number was calculated as

$$Re = \frac{\rho \cdot d \cdot V_{\infty}}{\mu} \quad (5.1.1),$$

with $\rho = 1.23 \text{ kg m}^{-3}$, $\mu = 1.79 \cdot 10^{-5} \text{ kg m}^{-1} \text{ s}^{-1}$, $d = 113 \text{ mm}$, and $V_{\infty} = 26.1, 25, 12.3 \text{ m s}^{-1}$ correspondingly. The resultant Reynold numbers were written in the table. For the first experiment,

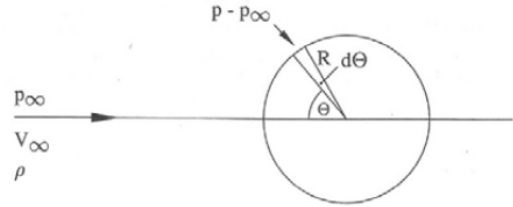
the mesh was used to increase Reynolds number. The actual Reynolds number would be higher than the calculated value, but it was not able to obtain.

In this experiment the pressure coefficients were all obtained by Matlab codings. In application, datas were entered where outputs were the pressure coefficients and the figure of angle versus pressure coefficient. Theoretical values were displayed in blue lines with equation (5.1.1) provided as

$$C_p = 1 - 4\sin^2\theta \quad (5.1.2).$$

It is sketched as the figure shown on the side about the flow geometry and the nomenclature. To do the free body diagram, it is clear to show that the drag acted on the slice dD is

$$dD = (p - p_\infty) \cdot R \cdot d\theta \cdot \cos\theta \quad (5.1.3).$$



It would be obvious that $d\theta \cdot \cos\theta = d\sin\theta$, therefore

$$dD = (p - p_\infty) \cdot R \cdot d\sin\theta.$$

Therefore

$$D = 2R \int_0^\pi p - p_\infty d\sin\theta \quad (5.1.4).$$

Recall equation (3.2)

$$C_p = \frac{p - p_\infty}{p_d} = \frac{p - p_\infty}{\frac{1}{2}\rho \cdot v_\infty^2},$$

and (3.1)

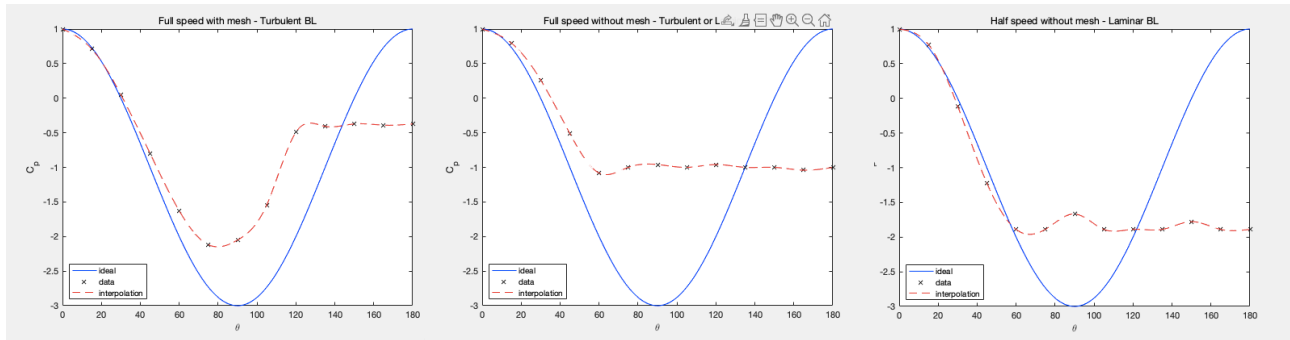
$$C_d = \frac{D}{\frac{1}{2}\rho \cdot v_\infty^2 \cdot l},$$

where $l = 2R$, thus finally

$$C_d = 2R \int_0^\pi C_p d\sin\theta \quad (5.1.5).$$

Logically a further graph of $\sin\theta$ versus pressure coefficient could also be obtained, where its area under the curve would be the value of drag coefficient. In this experiment, the drag coefficients were generated from the Matlab codes after typing the datas in. They were 0.28774, 1.1098, and 1.5685 correspondingly, shown in Table 5.1.1. The Matlab codes first calculated difference between all angle-measured data and free stream static pressure to get the normalized pressure readings. Second, datas were then interpolated and plotted. Third, drags were calculated. Finally area under the $\sin\theta$ curve was generated and calculated.

From the graphs, it is observed that as the angle increases, the pressure coefficient followed the path of the ideal values at first, then tended to decrease less than the ideal one. It rebounded and adjusted to a steady value. When the flow was in turbulent and had a fast rate, the final steady value



(approximately -0.5) is numerically higher than the average (ideally at -1). There was more region consumed to reach the final steady state, around 120° for turbulent versus that of 60° for laminar. For those of slow laminar flow were reversed. Since the Reynolds number itself is dependent on the flow velocity, the result implies that as the flow velocity rises, Reynolds number rises, therefore power coefficient rises numerically, as coefficient is dimensionless. According to the Figure 2.1, Reynolds number for second experiment was about $1.9 \cdot 10^5$, which would be turbulent flow.

In cylinder case, ideally, a laminar boundary layer should be formed around the cylinder and the flow is completely attached to the surface. In reality, the flow speed decreased when flowing around the cylinder, a stall occurred with the smooth transitions. As a result, the static pressure increased and the flow was experiencing a force in the opposite direction. The external streamlines imposed their pressure on the boundary layer and thus influenced the flowing path. The flow inside the boundary layer and in the undisturbed external flow influenced each other. This resulted in a recirculation area, which caused a flow separation.

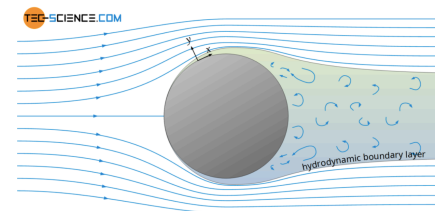


Figure 5.1.4 : Laminar flow around a cylinder with turbulent flow separation
<https://www.tec-science.com/mechanics/gases-and-liquids/>

Table 5.1.1 : Experiment A data table

Experiment	Meshed	Boundary Layer Condition	Wind Speed [m/s]	Drag Coefficient	Calculated Reynolds Number
1	Yes	Turbulent	26.1	0.28774	$2.0 \cdot 10^5$
2	No	Turbulent	25	1.1098	$1.9 \cdot 10^5$
3	No	Laminar	12.3	1.5685	$0.96 \cdot 10^5$

Compared to the theoretical data plotted, the first experiment has the smallest flow separation gap, around 60° for the tested region. But before the separation gap, there was significant difference between theoretical pressure coefficients and the practicals. For the last experiment, though there was a large separation gap, the variance of experimental datas was considered to be the smallest. Therefore it would be concluded that the third experiment was closest to theories.

5.2.Data Analysis of Part B

In this part the plots and output pressure coefficients were all obtained by Matlab codings. In application, datas were entered where outputs were the pressure coefficients and the figure of flow speed versus height. The outcome plots displayed the change in flow speed (blue line) compared

with the change in height, which shows the shape of the cylinder cross section. Pressure could be used by two different method, Trapezium Rule and Simpson Rule. In the experiments, both rules were applicable and the output was exactly the same. Therefore the Simpson Rule was used for both measurements.

Reynolds numbers for the two experiments were calculated by the relationship

$$C_d = \frac{\rho \cdot d \cdot V_\infty}{\mu}, \rho = 1.22 \text{ kg m}^{-3}, \mu = 1.8 \cdot 10^{-5} \text{ kg m}^{-1} \text{ s}^{-1}, d = 12 \text{ mm} \quad (5.2.1).$$

Derivation of the relationship between drag coefficient and flow velocity would be found in the *Foundations of Aerodynamics* listed in references. The final equation is listed as

$$C_d = \frac{1}{\frac{1}{2} \rho V_\infty^2 \cdot d} \int V(y) \cdot [V_\infty - V(y)] dy \quad (5.2.1).$$

Figure 5.2.1: Drag of a body from wake measurement

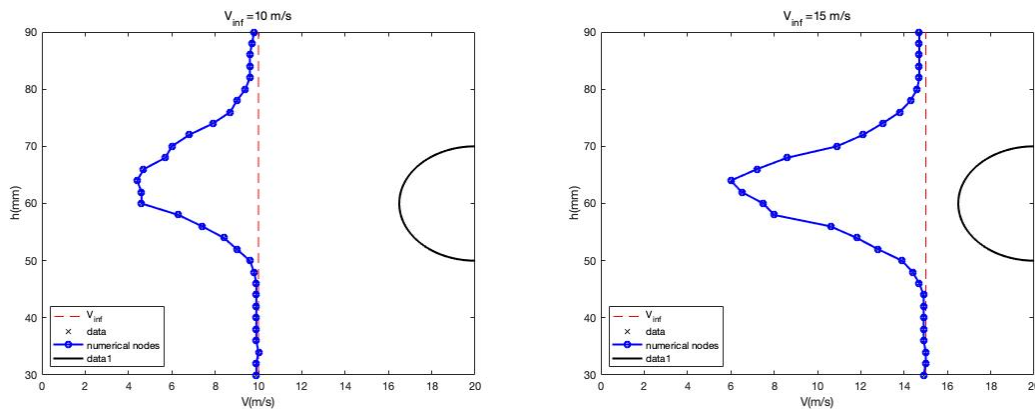


Figure 5.2.1 and 5.2.2: Matlab generated plots of two experiments in Section B, with axes measuring velocity versus height.

In the experiment the actual drag coefficients and Reynolds numbers were calculated and listed in Table 5.2.1. They were then compared with the graph in Figure 2.1: Drag coefficient for two-dimensional bodies. For the same Reynolds number, the theoretical drag coefficients were bigger than the actual calculated values.

Table 5.2.1 : Experiment B data table

Experiment	Wind Speed [m/s]	Reynolds Number	Drag Coefficient	Theoretical Drag Coefficient	Percentage of difference
1	15	12200	0.9479	1.3	27.1%
2	10	8133.3	1.0189	1.1	7.4%

The experimental uncertainty was lowered by choosing the maximum number of interpolation nodes, it could be improved by introducing the smooth interpolation curve to do the Matlab plotting and the calculation. Viscosity is numerically highly sensitive, so in the calculation 2 significant figures might not be accurate enough. For example given viscosity was $1.8 \cdot 10^{-5} \text{ kg m}^{-1} \text{ s}^{-1}$, whereas for assumed room temperature 20°C , the actual viscosity is $1.825 \cdot 10^{-5} \text{ kg m}^{-1} \text{ s}^{-1}$. In the wind tunnel the speed was fluctuating all the time. The manometer's reading scale was loaded far away from the actual measured height, therefore random error could be caused. The flows were all

turbulent, with Reynolds number all higher than 3000. In this case there might be boundary layer separation so that the velocity measured might not match the real speed of air flow, thus the measured data might have significant difference compared with actual flow speed. To overcome the effect, a fluid with lower viscosity must be used instead. It could be achieved by either decreasing the flow velocity, projected diameter, and density, or increasing the viscosity. In practice, use of slow air flow or hot air flow could be solving the issue.

For the minimum velocities, they were occurred at $y = 64\text{mm}$, with $V_{min1} = 6$ and $V_{min2} = 4.4$. Velocity ratios were

$$\frac{V_{min1}}{V_{\infty1}} = 6 \div 15 = 0.4, \frac{V_{min2}}{V_{\infty2}} = 4.4 \div 10 = 0.44.$$

The ratio between minimum velocities and maximums were considerably equal. The velocity loss was likely the same proportion. This would be explained as the model was the same, the wind energy loss would be proportional to the speed, thus the ratio would be equal.

The wake width would be the width where it did not behave regularly, as for the first experiment the data were following the trend until the height of 60mm. This relatively random and asymmetrical behavior lasted until height of 70mm reached. For the second experiment they were not following the trend from 58mm to 66mm. Therefore it could be concluded that the wake would be approximately 10mm for fast flow and 12mm for slow flow. For the first experiment the percentage of difference between actual and experimental value was too high (over 25%), and the relationship between Reynolds Number and drag coefficient should be positive but in experiment they were negative. System errors might be happening in the experiment as both values in 1 and 2 were lower than the theoretical values.

By theory, with a high Reynolds number, through turbulent flow, mixing high energy fluid was entrained into the boundary layer (the wake), boundary layer could therefore stay attached longer. As the speed of air increased, the wake was therefore smaller. This is happening where the sudden drop occurred in Figure 2.1. But in Part B, the Reynolds number was not higher enough to prove the theory, so the negative relationship would only be a measurement accident.

6. Conclusions

From part A it would be concluded that the drag coefficient of drag would be affected by the boundary layer conditions of the flow, if the flow is turbulent then drag coefficient would be lower and for laminar of that would be higher. In another perspective, for the same model, if the flow speed rises, drag coefficient decreases. For part B, as Reynolds number increase, drag coefficient decrease, although it did not obey the theory.

Thus there were imperfections in both parts, the errors have made the calculated Reynolds numbers, pressure coefficients and drag coefficients lower than actual values. But in general, the results were following the relationships, there might be improvements in the first experiment in part A, if wind tunnel had a higher speed limit, then the real Reynolds number would be calculated, and thus it could have better proving of the result.

7. Bibliography

‘Recommend readings.’ *Physical Fluid Dynamics (2nd Edition)*, Oxford Publications, Clarendon Press, 1988), D.J. Tritton. ISBN 978-0-12-482250-4, <https://doi.org/10.1016/B978-0-12-482250-4.X5001-2>

‘Definition of Streamline.’ *Merriam-Webster.com Dictionary*, Merriam-Webster, <https://www.merriam-webster.com/dictionary/streamline>. Accessed 20 Nov. 2020.

‘Reynolds Number.’ *Marine Propellers and Propulsion (Fourth Edition, 2019)*, J.S. Carlton, pages 47-57, ISBN 978-0-08-100366-4, <https://doi.org/10.1016/C2014-0-01177-X>.

‘Boundary Layer Separation.’ *Bioprocess Engineering Principles (Second Edition, 2013)*, Pauline M. Doran, Chapter 7 - Fluid Flow, Editor(s): Pauline M. Doran, Pages 201-254, ISBN 9780122208515, <https://doi.org/10.1016/B978-0-12-220851-5.00007-1>.

‘Skin Friction Drag, Pressure Drag, Drag Coefficient, Pressure Coefficient.’ *Drag coefficient (friction and pressure drag)*, tec-science, <https://www.tec-science.com/mechanics/gases-and-liquids/drag-coefficient-friction-and-pressure-drag>, 31 May. 2020.

‘Figure for Drag of a body from wake measurement.’ *Foundations of Aerodynamics (Fifth Edition, 1998)*, John Wiley & Sons, Kuethe, A.M., Chow, C.-Y. Example 3.7, pp.84–86, ISSN 0016-0032, [https://doi.org/10.1016/0016-0032\(51\)90591-1](https://doi.org/10.1016/0016-0032(51)90591-1).

‘Figure of Drag coefficient for two-dimensional bodies.’ *Mechanics of Fluids (seventh Edition, 1998)* B.S. Massey, revised by John Ward-Smith (Taylor&Francis.), ISBN 978-0748740437,